Article

Thermal Environment and Animal Comfort of Aviary Prototypes with Photovoltaic Solar Panel on the Roof

Charles Paranhos Oliveira [1,*] **, Fernanda Campos de Sousa** [1] **, Gabriel Machado Dallago** [2] **, Jocássia Reis Silva** [1] **, Paulo Henrique Reis Furtado Campos** [3] **, Maria Clara de Carvalho Guimarães** [4] **and Fernando da Costa Baêta** [1]

1   Department of Agricultural Engineering, Universidade Federal de Viçosa, Viçosa 36570-900, MG, Brazil
2   Animal Science Department, McGill University, Sainte-Anne-de-Bellevue, QC H9X 3V9, Canada
3   Department of Animal Science, Universidade Federal de Viçosa, Viçosa 36570-900, MG, Brazil
4   Department of Agronomy, Universidade Federal dos Vales do Jequitinhonha e Mucuri,
    Diamantina 39100-000, MG, Brazil
*   Correspondence: charles.paranhos@ufv.br

Abstract: The areas on the roofs of animal production facilities present great potential for generating solar energy. However, the impact that the addition of new material on the roof can generate on the installation's thermal environment is still poorly studied. Thus, this study aims to investigate the effect of the application of photovoltaic panels in the roofs of prototypes, in reduced-scale aviaries, on the thermal environment, and on the animal comfort condition inside the prototypes. For this, six prototypes of aviaries on a reduced 1:5 scale are used. They are equipped with three types of tiles (ceramic, fiber-cement, and metal), with and without a photovoltaic panel. The effect of applying the photovoltaic panel is verified by evaluating the air temperature, the surface temperature of the roofs, the temperature and humidity index (THI), the black globe humidity index (BGHI), and the radiation heat load (RHL). The results show that applying the photovoltaic panel on the roof, regardless of the type of tile, is efficient in reducing the air temperature by about 0.4 °C, the BGHI by about 0.7, and the RHL about 4 W/m². As for THI, there is only a 4.8 reduction in fiber-cement roofs.

Keywords: thermal comfort and solar energy; solar energy in rural environment; thermal comfort assessment; solar energy in rural environment

1. Introduction

The roof areas of the facilities used for the confinement of animals in animal-production agroindustry, as well as the aviaries for producing broilers, have a high potential for generating photovoltaic energy. This is due to the high incidence of solar radiation, given the orientation of the installations, and the possibility of making better use of this previously available area. Therefore, the use of photovoltaic panels on the roof of installations has become increasingly present in the reality of Brazilian producers and tends to increase because of the need to make animal production systems more sustainable and energetically autonomous. In addition, the use of renewable energies tends to increase in all sectors because of the commitment made by Brazil in the Paris Agreement, which should generate tax incentives for the development of more sustainable technologies [1].

The application of photovoltaic panels on buildings consists of the association of photovoltaic modules to the constructive elements of the structure, most being applied on the roofs [2,3]. This application can generate impacts on the thermal environment of the facility and affect one of the main objectives of the roof, which is to reduce the radiation that reaches the interior of the building, to maintain the range of animal thermal comfort within what is considered ideal. The shading conferred and the total thermal radiation that reaches the interior of the facilities depend mainly on the materials that are used in the construction of the roof [4,5]. There are already some studies on the effects of the use of photovoltaic panels positioned on the roof, above the cooling and heating loads of the top

floor of urban buildings [6–9], a considerable reduction in the requirements of cooling loads being verified [8–12]. This reduction is attributed to the lower heat flow from the outside to the inside of the roof [13–16], which contributed to reduce the internal temperature [8,17]. This fact represents a great advantage for Brazilian animal production systems, especially in summer, when they demand a large amount of energy to keep ventilation systems in operation to maintain animal thermal comfort inside the facility.

The ventilation demand in the aviaries is mainly due to the need to reduce the temperature of the internal air, since the production animals are homeothermic; that is, they have the ability to maintain the temperature of their body core within a narrow temperature limit that allows vital functions to remain active [18]. Thus, when the temperature of the environment reaches values characterized as stressors, above or below the limits established as thermal comfort, the physiological processes that increase or decrease the animal's internal body temperature are activated, which results in worse performance.

To assess the degree of thermal comfort in animal production facilities, indices of the thermal environment are normally used. They satisfactorily indicate the thermal sensation of the animal housed in the construction and can be used in the evaluation of the thermal efficiency of roofing materials [5,19–21]. These indexes relate the environmental variables and consider the animal–environment heat exchange, this being an excellent indicator of the animal's thermal condition. In this sense, the authors of a study carried out in central Europe observed a reduction of 2.8 in the temperature and humidity index of reduced-scale prototypes and barns in real conditions with metallic cover associated with the application of photovoltaic modules on the cover [20]. In another study carried out in Brazil, using photovoltaic modules as a shading alternative for sheep and lambs, a 40 W/m^2 reduction in the thermal radiation load was observed in relation to the use of a mesh with 80% shading [22]. This study also showed that the ewes and lambs preferred, 70% of the time, to be under the shade generated by the photovoltaic modules.

It is observed that there are several studies evaluating the energy demand of urban buildings with the use of photovoltaic panels in the envelope or roof. However, studies using photovoltaic panels on the roofs of rural buildings are still scarce. In this sense, this study aims to complement the existing literature on the effects of using photovoltaic panels on rural buildings with the combination of different types of tiles on the thermal environment and animal comfort. To meet this objective, an experiment was set up using small-scale aviary prototypes with the combination of photovoltaic panels with three types of tiles in a hot climate region.

2. Materials and Methods

The research was carried out in six prototypes of aviaries present in the facilities of the Nucleus for Research in Ambience and Engineering of Agroindustrial Systems (AMBIAGRO), of the Department of Agricultural Engineering at the Universidade Federal de Viçosa (UFV) in Viçosa, MG. The prototypes are located at the following coordinates: latitude 20°46′17″ S and longitude 42°52′21″ W, with an average altitude of 670 m. The climate of the region, according to the Köppen classification, is Cwa, a subtropical climate with dry and cold winters and hot and humid summers. The experiment was conducted during the hottest time of the year, between the months of November and December 2020.

The six prototypes used were created in reduced scales of a commercial broiler's aviary, using the concept of similarity in the scale 1:5 [23,24]. All prototypes have the same dimensions of 2.5 m in width, 3.2 m in length, 0.6 m of ceiling height, and 0.95 m of ridge height. They were positioned in a flat, grassy area, distributed in two lines, with the ridge oriented in the east–west direction. The prototypes were placed with 6 m between them in the longitudinal direction and 8 m of distance between the lines (Figure 1).

The prototypes used represent hybrid poultry facilities with a natural ventilation system on the north/south sides that remain predominantly open. The east/west sides, which represent the gablets of the installation, were closed with 0.01 m thick plywood boards. The roof consists of two waters with a slope of 30%. The supporting structure of the

prototypes is modular, every 0.80 m with pillars with a square section of 0.03 m × 0.03 m. The floor consists of 0.01 m plywood boards, 0.40 m from the ground and supported by wooden beams, in the transverse direction, with a rectangular section of 0.03 m × 0.05 m. The roof structure is made of wood, consisting of two beams in the longitudinal direction, with a rectangular section of 0.03 m × 0.05 m positioned on the sides and a ridge beam with a rectangular section of 0.04 m × 0.10 m.
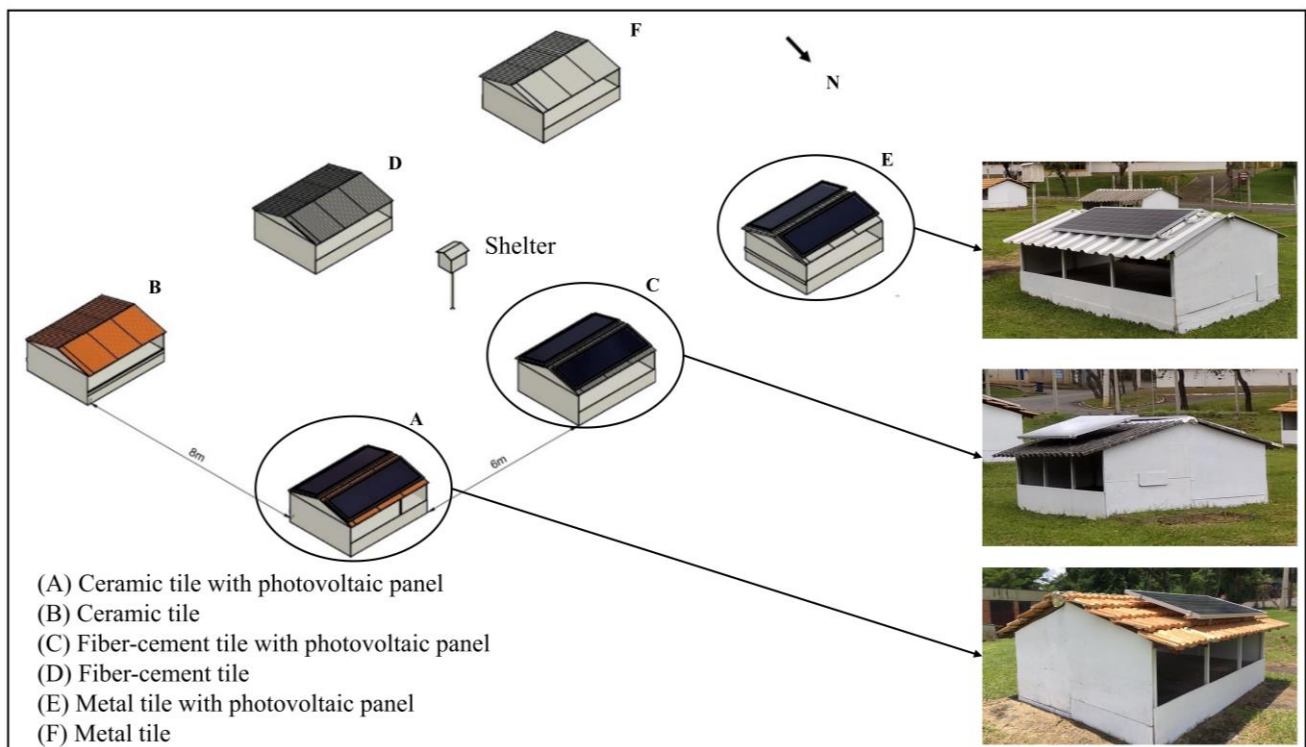

Figure 1. Sketch of the layout of prototypes and treatments.

The treatments consisted of the use of three different combinations of roofing materials with the absence and presence of a photovoltaic panel. The types of tiles used were Roman ceramic tile, corrugated fiber-cement tiles, 5.0 mm thickness, and metal tile in a trapezoidal shape, 0.4 mm thickness. Three of the six prototypes were equipped with two photovoltaic panels with polycrystalline silicon cells, one in each roof water, with the dimensions of 2 m long and 1 m wide, covering 53% of the roof. The panels were positioned 0.1 m from the roofs on ceramic and fiber-cement tiles and 0.05 m on metal tile, all inclined toward the north and south sides; these distances were chosen considering the standard of commercial installation for each type of roof tile.

2.1. Effect of the Photovoltaic Solar Panel on the Prototype's Thermal Environment

For the analysis of the thermal environment of the prototypes, continuous data referring to the air temperature (°C) were monitored inside the prototypes. Temperature data were collected continuously and recorded at 15 min intervals, using a HOBO brand datalogger, model U14-001, with a accuracy of ±0.21 °C (temperature) and ±2.5% (humidity), installed in the geometric center of each prototype at 0.3 m high. All equipment used in this study underwent a sensitivity test, having been compared in an environment with controlled temperature and their errors estimated.

For the assessment of thermal comfort, the observed air temperature values were compared with the thermoneutrality ranges present in the literature, as shown in Table 1.

For the thermal analysis of the prototype's roofing materials, the internal surface temperature of the tile (IST) was determined using a Fluke infrared thermometer, model 62 MAX+, with an accuracy of ±1 °C, according to the methodology proposed by

Eckelkamp et al. [25]. Surface temperature data were collected daily at three-hour intervals, between 6:00 and 18:00 h, throughout the experimental period.

Table 1. Thermoneutrality range for broilers.

| Author (Year) | Thermoneutrality Range in the Weeks of the Broiler Production Cycle (°C) | | | |
	1	2	3	4
Cassuce et al. [26]	31.3	26.3–27.1	22.5–23.2	-
Abreu and Abreu [27]	32.0–35.0	29.0–32.0	26.0–29.0	23.0–26.0

Thermographic images were obtained by a portable thermographic camera coupled to a cell phone of the brand Flir, model FLIR ONE Pro, with a measurement range of -20 to $400\ °C$ and precision of $\pm 3.0\ °C$, with the images obtained at 12:00 (time of greatest solar radiation intensity) and 15:00 h (most critical time inside the prototypes).

2.2. Effect of a Photovoltaic Panel on Animal Thermal Comfort

The effects of the presence of the photovoltaic solar panel on the animal thermal comfort condition were evaluated through the determination of indices related to the thermal environment of the installation and to the animal's comfort condition.

The temperature and humidity index (THI) was estimated according to the model developed by Thom [28] cited by [18] based on Equation (1).

$$\text{THI} = 0.72(\text{T}_\text{d} + \text{T}_\text{w}) + 40.6 \qquad (1)$$

where T_d represents dry bulb temperature (°C) and T_w, wet bulb temperature (°C).

It was determined the black globe humidity index (BGHI), developed by Buffington et al. [29], which incorporates all climatic factors indirectly (temperature, relative humidity, air velocity, and radiation) in a single value that was estimated by Equation (2).

$$\text{BGHI} = \text{T}_\text{bg} + 0.36\ \text{T}_\text{dp} + 41.5 \qquad (2)$$

where T_bg represents black globe temperature (°C) and T_dp, dew point temperature (°C).

Radiant exchanges at the animals' level were quantified by radiation heat load (RHL) (Equation (3)), with calculation based on the mean radiant temperature (MRT), represented by Equation (4) [30].

$$\text{RHL} = \sigma\ (\text{MRT})^4 \qquad (3)$$

where σ represents the Stefan-Boltzmann constant ($5.67 \times 10^{-8}\ \text{W m}^{-2}\ \text{K}^{-4}$) and MRT (K).

$$\text{MRT} = 100\left[2.51\ \sqrt{V}\ (\text{T}_\text{g} - \text{T}_\text{s}) + (\text{T}_\text{g}/100)^4\right]^{1/4} \qquad (4)$$

where V is the airspeed (m s^{-1}), T_g, the black globe temperature (K), and T_s, the dry bulb temperature (K).

For the evaluation of animal thermal comfort, the calculated values of THI and BGHI were compared with the comfort ranges available in the literature, as shown in Table 2.

For the index's composition, relative air humidity (%), black globe temperature (°C), and air speed (m/s) were monitored inside the prototypes. Relative air humidity data were collected continuously and recorded at 15 min intervals using a HOBO brand datalogger, model U14-001, with a accuracy of $\pm 0.21\ °C$ (temperature) and $\pm 2.5\%$ (moisture), installed in the geometric center of each prototype.

To determine the temperature of the black globe we used Hobo sensors, model UX100-003, with a measuring range of $-20\ °C$ to $+70\ °C$, accuracy of $\pm 0.21\ °C$, placed inside plastic globes of the polyvinyl chloride (PVC) with 15 cm diameter, double painted in matte

black paint. The globes with the HOBOs were installed in the geometric center of each prototype and inside the meteorological shelter.

Table 2. Thermal comfort bands for broilers from the first to the fourth week of life.

Week of Life	Comfort Range	
	THI	**BGHI**
1	72.4–80.0	81.3
2	68.4–76.0	74.9
3	64.5–72.0	69.8
4	60.5–68.0	69.8
Source	Silva et al. [31]	Oliveira et al. [32]

Air velocity was measured using a hot wire anemometer, brand Instrutherm, model TAFR200, with an accuracy of ±3%. Air velocity data were collected inside the prototype, on the north and south sides, daily at three-hour intervals, between 6:00 and 18:00 h, throughout the experimental period.

2.3. Statistical Analysis

Statistical analyses were conducted using the R program [33], considering the level of statistical significance $\alpha < 0.05$ for all tests. The mixed effect statistical model presented in Equation (5) was used in the analyses, considering the repeated measures in time.

$$Y_{jkmn} = \mu + D_j + H_{kj} + T_{mj} + P_{nj} + (HT)_{kmj} + (HP)_{knj} + (TP)_{mnj} + (HTP)_{kmnj} + \varepsilon_{jkmn} \qquad (5)$$

where μ represents the overall mean, D_j represents the random effect of the j-th day$\sim N(0, \sigma^2)$, H_{kj} represents the effect of the k-th hour (6, 9, 12, 15 and 18), T_{mj} represents the effect of the m-th tile (ceramic, fiber-cement and metallic), P_{nj} represents the effect of the n-th panel (present and absent), $(HT)_{kmj}$ represents the interaction between hour and tile, $(HP)_{knj}$ represents the interaction between hour and panel, $(TP)_{mnj}$ represents the interaction between tile and panel, $(HTP)_{kmnj}$ represents the interaction between hour, tile and panel, and ε_{jkmn} represents the experimental error$\sim N(0, \sigma^2)$.

Following the graphic procedures described by Pinheiro and Bates [34], the residues were analyzed to evaluate the fulfillment of the assumptions of normality, homoscedasticity, and independence. Still following the procedures described by Pinheiro and Bates [34], the random effect estimates were also evaluated in terms of compliance with normality and independence. Observing no homoscedasticity, the structure of the covariance matrix was then modeled using a variance model allowing different variances at each stratification level. Time, tile, panel, day, and day × time were evaluated as stratification variables. The Akaike information criteria (AIC) was used as a criterion for selecting the model that best fitted the data. Marginal means were compared for statistically significant effects, using the Bonferroni adjustment for multiple comparisons.

3. Results and Discussion

3.1. Effect of the Photovoltaic Panel on the Thermal Environment of the Prototypes

3.1.1. Air Temperature Inside the Prototypes

By the results of the analysis of variance, it was verified that for the air temperature there was no interaction between the treatments photovoltaic panel, tile and time. However, the F test showed that the comparison between the absence and presence of the photovoltaic panel is significant regardless of the type of tile used. (p-value = 0.006). Thus, regardless the type of tile and the time of day, the marginal averages were 27.4 ± 0.2 °C for the absence of the photovoltaic panel and 27.0 ± 0.2 °C for the presence of the photovoltaic panel, which represents a reduction of about 0.4 °C in the application of the photovoltaic panel

in relation to conventional roofs. This difference is due to the fact that the presence of the photovoltaic panel on the roof increases the insulating layer (panel, air gap, and tile) of the roof and reduces the heat flow from the external environment to the internal environment, which can affect the internal temperature of the environment [13,16].

It was verified in the analysis of variance that there was an interaction between the type of tile and the time (*p*-value < 0.001), being the fiber-cement tile statistically different from the ceramic and metallic tiles. This result can be explained by the fact that ceramic tiles are materials with greater efficiency in thermal insulation when compared to fiber-cement and metallic tiles [35–38]. In addition, metal tiles are highly reflective compared to fiber-cement and ceramic tiles [39] and when new they have a thermal performance similar to ceramic tiles [5,37,40]. These differences were mainly observed at 12:00 and 15:00 h, when the values of the external temperature are higher because of the occurrence of greater intensity of solar radiation on the roofs of the prototypes.

The behavior of the air temperature values inside the prototypes with ceramic, fiber-cement, and metallic tile, with the presence and absence of a photovoltaic panel on the roof, are shown in Figure 2.
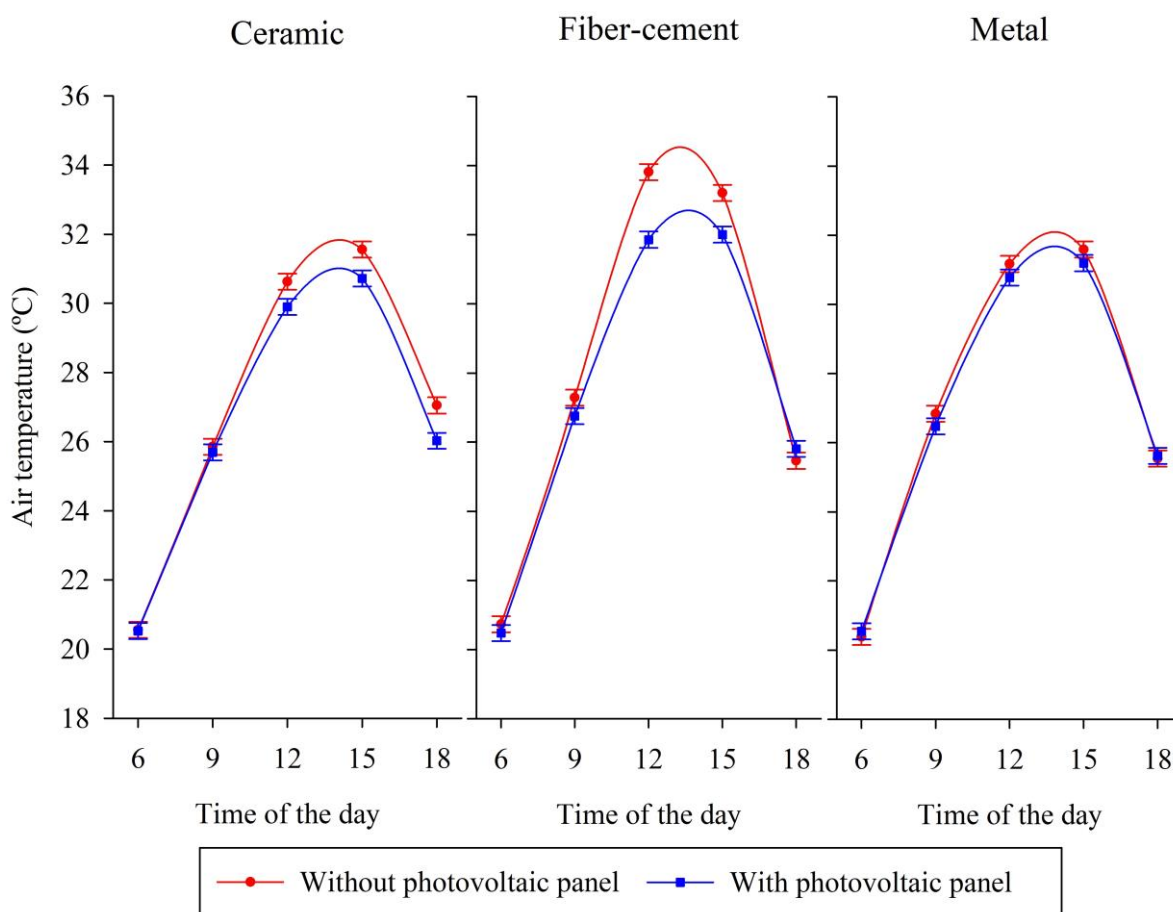

Figure 2. Behavior of the air temperature values inside the prototypes with the three types of tiles (ceramic, fiber-cement, and metallic) with the absence and presence of the photovoltaic panel.

It is observed in Figure 2 that the air temperature for all types of tiles analyzed was higher at the hottest times of the day, between 12:00 and 15:00 h, especially in the case of roofs without the application of the photovoltaic panel. In the prototypes with ceramic tile, the average value of air temperature at 12:00 h was 30.6 °C and at 15:00 h it was 31.6 °C, while in the prototypes with ceramic tiles and photovoltaic panels these values were 29.9 and 30.7 °C, respectively. The differences in air temperature values between the prototypes with the absence and presence of a photovoltaic panel were around 0.7 °C at 12:00 and

around 0.8 °C at 15:00 h. In the prototypes with ceramic tile, there was a particularity, in relation to the other types of tiles tested, where at 18:00 h there was a difference of about 1.0 °C between the absence and presence of the photovoltaic panel, which can be attributed to the shade generated by the photovoltaic panel, which increased its thermal inertia.

The highest air temperature values were found in the prototype with fiber-cement tile, where values of 33.8 and 33.2 °C were recorded at 12:00 and 15:00 h, respectively. In the association of fiber-cement tile with the photovoltaic panel, these values were 31.9 and 32.0 °C, respectively (Figure 2). Therefore, the differences between the air temperature values in the prototypes with fiber-cement tile with the absence and presence of the photovoltaic panel were about 2.0 °C at 12:00 and about 1.2 °C at 15:00 h. These values corroborate the values found by Bonifacius and Ekasiwi [41] who, when comparing a fiber-cement roof with a photovoltaic roof in prototypes, in Indonesia, observed a reduction in the range of 1.1 to 1.2 °C in the air temperature, at the times hottest of the day.

In the prototypes with metallic tile, the air temperature at 12:00 h was 31.2 °C and at 15:00 h it reached 31.6 °C; in the prototypes with metallic tile and photovoltaic panels, these values were 30.8 and 31.2 °C, respectively (Figure 2). In the prototypes with metal roofs, the differences in air temperature values between the absence and presence of the photovoltaic panel at 12:00 and at 15:00 h were the same, with a reduction of about 0.4 °C observed in the prototypes with the presence of the photovoltaic panels. However, Bilčík et al. [20] studying the effect of the photovoltaic panel in association with metallic tile in prototypes of barns completely closed on the sides in MDF and real barns in Central European conditions, observed a reduction of about 1.2 °C in those with the application of photovoltaic panels. In our study, it was found a value three times lower for the metallic roof (0.4 °C); this can be attributed to the fact that the prototypes of the present study have their sides opened, which enhances natural ventilation and air renewal, leaving the internal environment more susceptible to external conditions.

In the evaluation of thermal comfort, all treatments were above the thermoneutral range, which is 23 to 26 °C for broilers in the fourth week of life at the hottest times of the day (Table 1) [27]. The application of the photovoltaic panel on the roof was not enough to reduce the internal ambient temperature and keep the microclimate within the comfort range. However, when considering the second week of life of birds that require heating, the application of the photovoltaic panel on the fiber-cement tile was enough to reduce the temperature of the internal environment to the thermoneutral range, which is 31.5 to 35 °C [26,27].

3.1.2. Surface Temperatures of the Prototype Roofs

The behavior of the internal surface temperature of the tiles and the analysis of variance for the three types of tiles, with and without photovoltaic panel, are shown in Figure 3.

The values of the internal surface temperatures of the tiles for the absence and presence of the photovoltaic panel showed similar behavior for the three types of tiles (Figure 3). Nevertheless, it was verified that there was a greater reduction in the internal surface temperature in the fiber-cement tiles, when compared to the absence and presence of photovoltaic panels. At 9:00 h, they were observed mean values of 37.6 ± 0.8 °C on the roof without panel and 29.5 ± 0.8 °C on the roof with panel (p-value < 0.001), at 12:00 h they were observed mean values of 49.6 ± 0.8 °C in the roof without panel and 37.0 ± 0.8 °C in the roof with panel (p-value < 0.001) and at 15:00 h, mean values of 43.4 ± 0.8 °C on the roof without panel and 35.0 ± 0.8 °C on the roof with panel (p-value < 0.001). Thus, the differences between the values of the internal surface temperatures of the fiber-cement roofs with and without panel were around 8.0, 12.6, and 8.4 °C, for 9:00, 12:00, and 15:00 h, respectively.

In metal roofs, it was verified (Figure 3) that the internal surface temperature was significantly higher in the roof without a photovoltaic panel at 12:00 h, with an average value of 37.9 ± 0.8 °C, when compared to the roofs with the photovoltaic panels with an average value of 32.0 ± 0.8 °C (p-value = 0.003), which represents a reduction of about 5.5 °C. On the other hand, in ceramic tiles, no significant differences were observed in the

values of the internal surface temperature of the roofs with the absence and presence of photovoltaic panels., although the chart shows a reduction of around 3.0 °C. This may be due to the insulating characteristic of ceramic tile, as it is considered a high-efficiency thermal insulator, especially in comparison with the other materials tested [36].
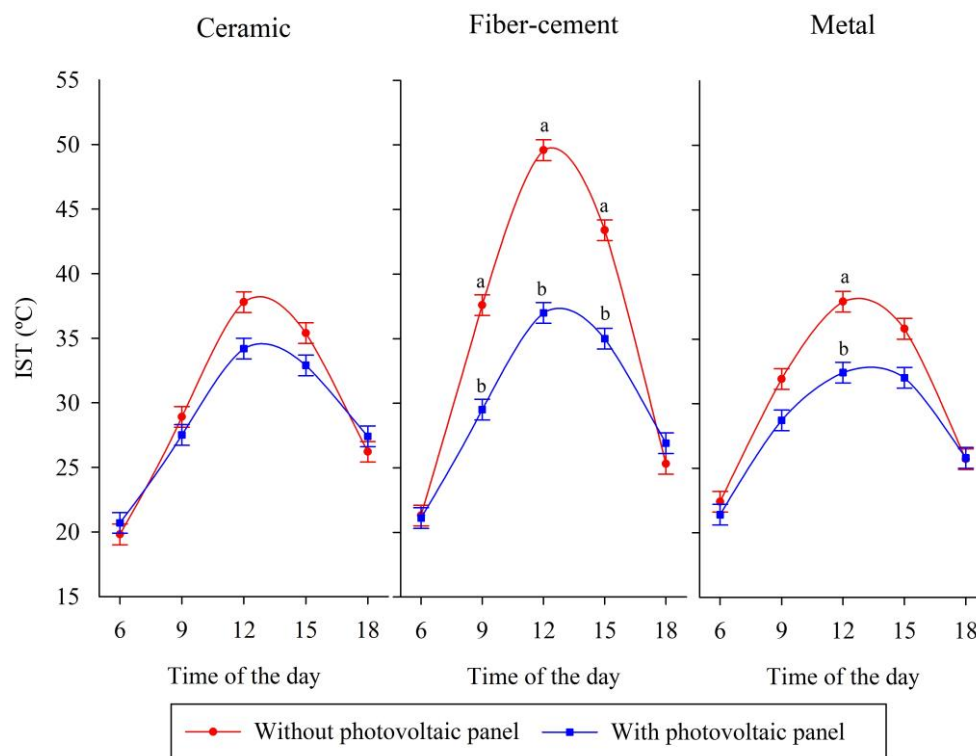

Figure 3. Behavior of the internal surface temperature (IST) values of the tiles and the unfolding of the interaction between the absence and presence of the photovoltaic panel for the three types of tiles analyzed within the hours. Different letters indicate that the values are statistically different, and the absence of the letter indicates that there were no significant differences.

Our results corroborate those found by Dominguez et al. [13], who found a reduction in the internal surface temperature of the roof when the photovoltaic panel was associated with the roof of a building in climatic conditions in California, in the United States. The authors performed the thermal modeling of the profile with the photovoltaic modules and without the modules. In the region with an inclined panel, a reduction of about 63% of the heat flux and a reduction in the cooling loads was verified in comparison with the region without photovoltaic panel [13]. This may represent lower energy expenditure to cool aviaries in Brazil during the hot periods of the year, which require ventilation throughout the day to provide microclimatic conditions of thermal comfort to the animals and ensure that they express their maximum genetic potential.

Figures 4 and 5 show the thermographic images of the prototypes with the different types of tiles and with the presence and absence of photovoltaic panels, at 12:00 and 15:00 h, respectively. As can be seen from the images, temperatures on the external surface were relatively high, with the highest value observed in the fiber-cement tile at 12:00 h with 56.5 °C (Figure 4d), the ceramic tile with 45.7 °C (Figure 4b), and the metallic tile with 26.2 °C (Figure 4f). This high surface temperature in fiber-cement tile can be explained by the higher absorption of solar radiation in relation to ceramic and metallic tile and the low surface temperature of metallic tile can be explained by its high reflective capacity [39].

It is observed that the temperatures on the surface of the photovoltaic panel on the metallic cover were slightly higher (Figures 4 and 5) in relation to the other covers with the presence of the photovoltaic panel. With the highest value recorded at 12:00 h, with a value of 51.6 °C (Figure 4e), in the ceramic covering the surface temperature of the panel

was 41.0 °C (Figure 4a) and in the fiber-cement covering of 44.9 °C (Figure 4c). The surface temperature of the panel on the metal tile was slightly higher because of the proximity of the panel to the tile (air gap of 5 cm), which reduces convection heat exchanges [42]. Module efficiency is directly related to panel temperature. A 1 °C increase in temperature above 25 °C impairs efficiency by about 0.4% [43–45].
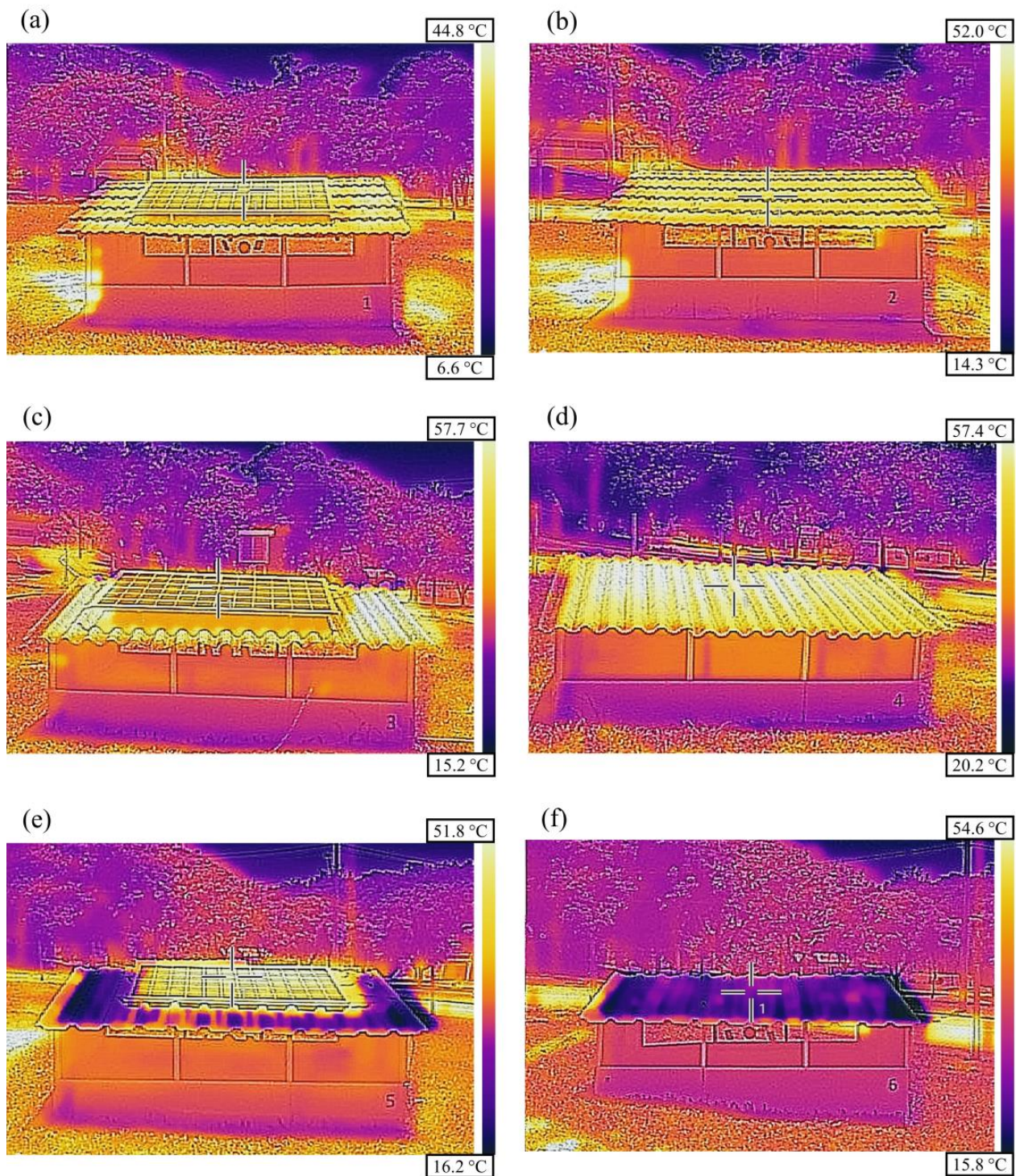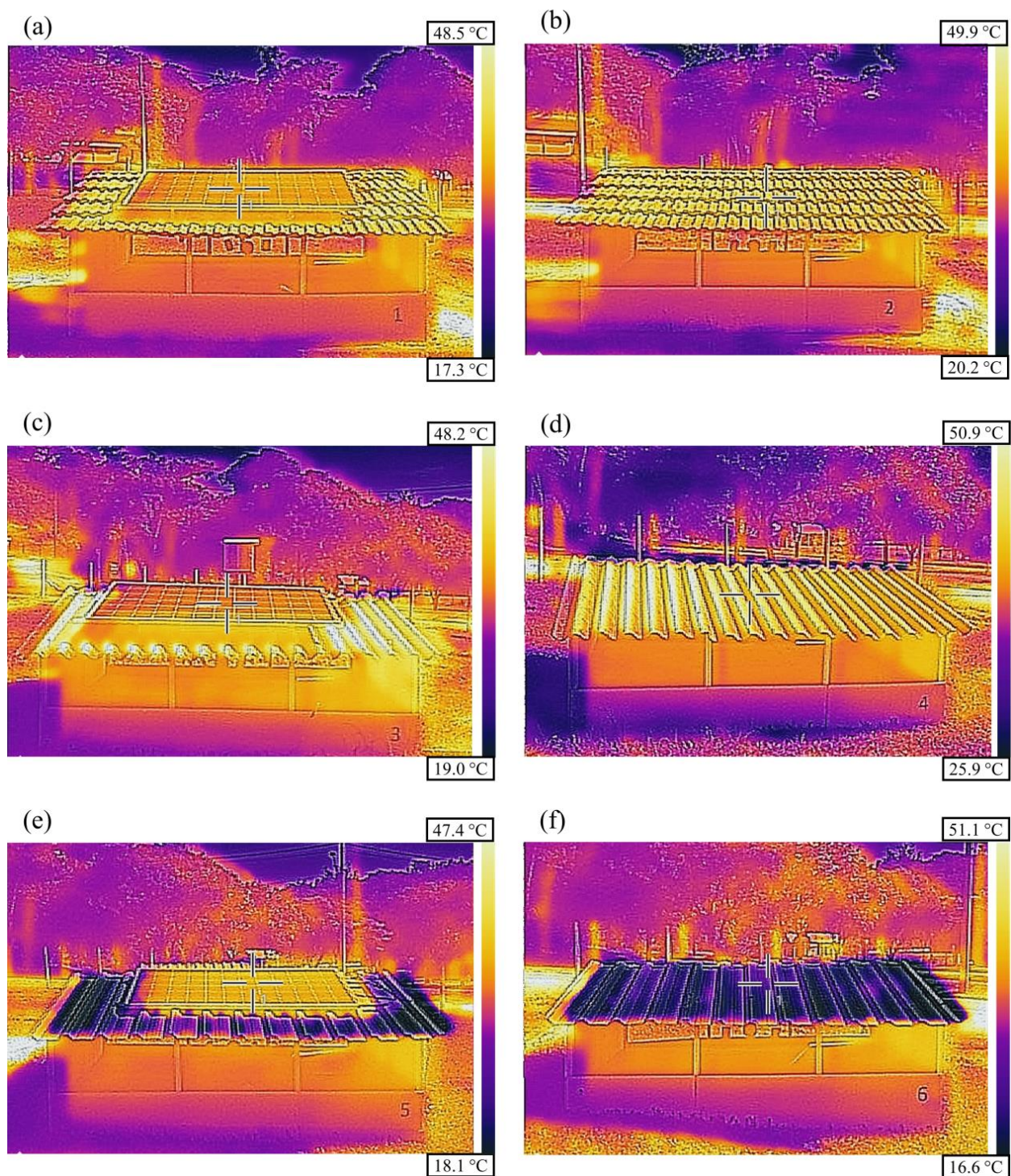

Figure 4. Infrared thermography of the prototypes at 12:00 h: (**a**) ceramic tile with photovoltaic panel; (**b**) ceramic tile; (**c**) fiber-cement tile with photovoltaic panel; (**d**) fiber-cement tile; (**e**) metallic tile with photovoltaic panel; and (**f**) metallic tile.

Figure 5. Infrared thermography of the prototypes at 15:00 h: (**a**) ceramic tile with photovoltaic panel; (**b**) ceramic tile; (**c**) fiber-cement tile with photovoltaic panel; (**d**) fiber-cement tile; (**e**) metallic tile with photovoltaic panel; and (**f**) metallic tile.

3.2. Effect of the Photovoltaic Panel on the Thermal Comfort of the Prototypes

3.2.1. Temperature and Humidity Index (THI)

The behavior of the THI values and the results of the analysis of variance for the prototypes with the three types of tiles tested, with and without the photovoltaic panel, are presented in Figure 6. It is observed that the highest values of THI were observed in the hottest moments of the day, between 12:00 and 15:00 h.
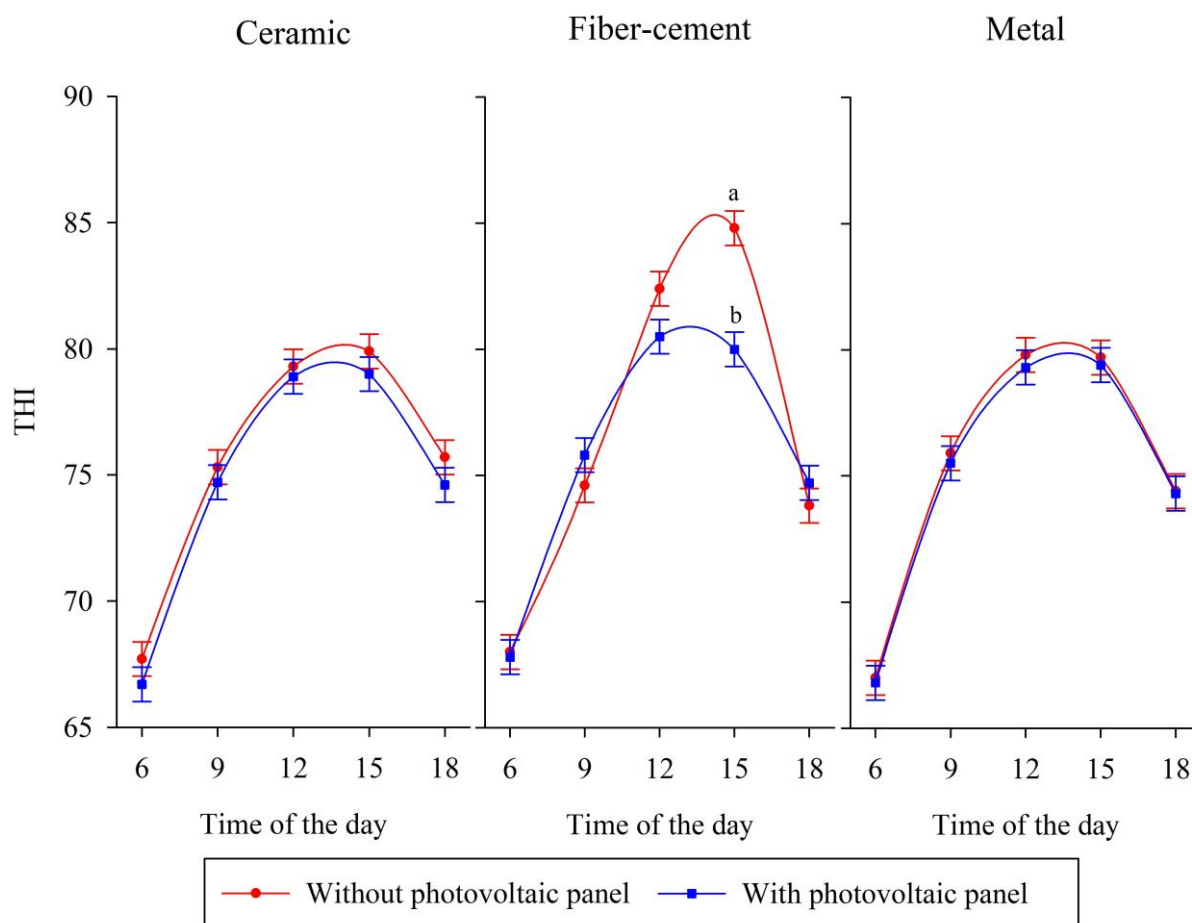
Figure 6. Behavior of the temperature and humidity index (THI) and unfolding of the interaction between the absence and presence of the photovoltaic panel for the three types of tiles analyzed within the hours. Different letters indicate that the values are statistically different, and the absence of a letter indicates that there were no significant differences.

By the analysis of variance, it was verified that there were significant differences in the THI values in the fiber-cement tile prototypes, comparing the absence and presence of the photovoltaic panel (Figure 6). The highest THI values were found in the prototypes with fiber-cement roof, where at 15:00 h it was calculated 84.8 ± 0.7, which significantly differed (p-value < 0.001) from the fiber-cement tile with photovoltaic panel, with THI of 80 ± 0.7, the difference being around 4.8 at this time. In the prototypes with ceramic and metallic roofs, there were no significant differences between the absence and presence of a photovoltaic panel. However, Bilčík et al. [20] observed a reduction of 2.8 in the THI value between metallic tiles and metallic tile associated with photovoltaic panel in prototypes with MDF closure. Comparing the results, the contrary finding in the present study was probably due to the occurrence of natural ventilation in the prototypes, which favored air renewal and made the internal environment of the prototypes more vulnerable to the same external conditions.

As there was interaction between the THI values in the prototypes with and without photovoltaic panel, the unfolding of this interaction is shown in Figure 7.

It can be seen from Figure 7 that in the prototypes with the absence of the photovoltaic panel, the calculated value of THI for the prototype with fiber-cement tile at 15:00 h differed statistically from the prototypes with ceramic and metallic tiles (p-value < 0.001). The application of the photovoltaic panel was efficient to reduce the THI in the prototype with fiber-cement roof because the values observed in the prototypes with the presence of the photovoltaic panel were the same for the three types of tiles analyzed.
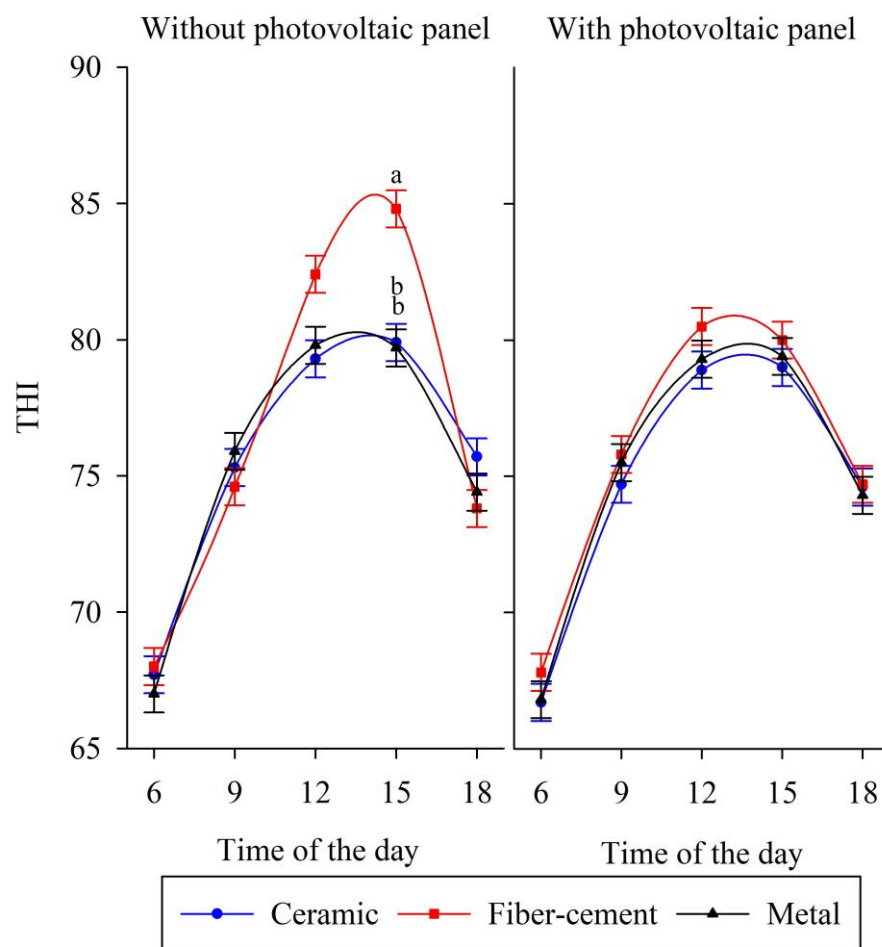
Figure 7. Behavior of the temperature and humidity index (THI) and the unfolding of the interaction between the three types of tiles analyzed within the hours, with and without photovoltaic panel. The different letters are statistically different, with the absence of a letter there were no significant differences.

The behavior of fiber-cement tile can be explained by its high value of absorption coefficient $\alpha = 0.7$, absorbing a considerable amount of radiation and, in addition, it has a coefficient of thermal conductivity of 0.76 W(m °C)$^{-1}$, but due to their reduced thickness (5 mm) they have low resistance to heat transmission [46]. This causes fiber-cement tiles to have high values of internal surface temperature, which directly impacts the values of air temperature and THI. On the other hand, new metallic tiles have a low absorption coefficient $\alpha = 0.2$, which makes them absorb little solar radiation [46]. At 18:00, it is observed that the THI values for the prototype with fiber-cement tile with photovoltaic panel is slightly higher than the THI for the fiber-cement tile. This was due to the addition of the photovoltaic panel, which may have increased the thermal resistance and the damping capacity of the roof [5,46]. The same was not observed for the other tiles, probably because they have good thermal characteristics [5,46].

The THI thermal comfort ranges for broilers are from 72.4 to 80 in the first week, 68.4 to 76 in the second week, 64.5 to 72 in the third week, and, for the adult phase, from 60.5 to 68 (Table 2) [31]. Thus, among the analyzed treatments, in the prototypes with fiber-cement roofs, THI values were observed, which represent a heat stress condition, for the first week of the lives of broilers. As for the adult phase, in all prototypes, in the hottest hours of the day, THI values were observed that characterize a heat stress condition.

3.2.2. Black Globe Humidity Index (BGHI)

By the analysis of variance, the values of BGHI were significantly lower in the prototypes with the application of the photovoltaic panel, presenting similar behaviors regardless of the type of tile and the time of day. Thus, the values of the marginal averages confused between tile type and hours were 76.4 ± 0.3 for the absence of a photovoltaic panel and 75.7 ± 0.3 for the presence of a photovoltaic panel, with a reduction in the value of the BGHI of about 0.7 (p-value = 0.001). The BGHI values showed an interaction between tile type and time (p-value < 0.001). The calculated values of BGHI in the prototypes with fiber-cement tile at the hours of 12:00 and 15:00 h were significantly higher in relation to the prototypes with metallic and ceramic tile at the same times.

The behavior of the BGHI values for the three types of tiles analyzed (ceramic, fiber-cement, and metal) with and without photovoltaic panel are presented in Figure 8.
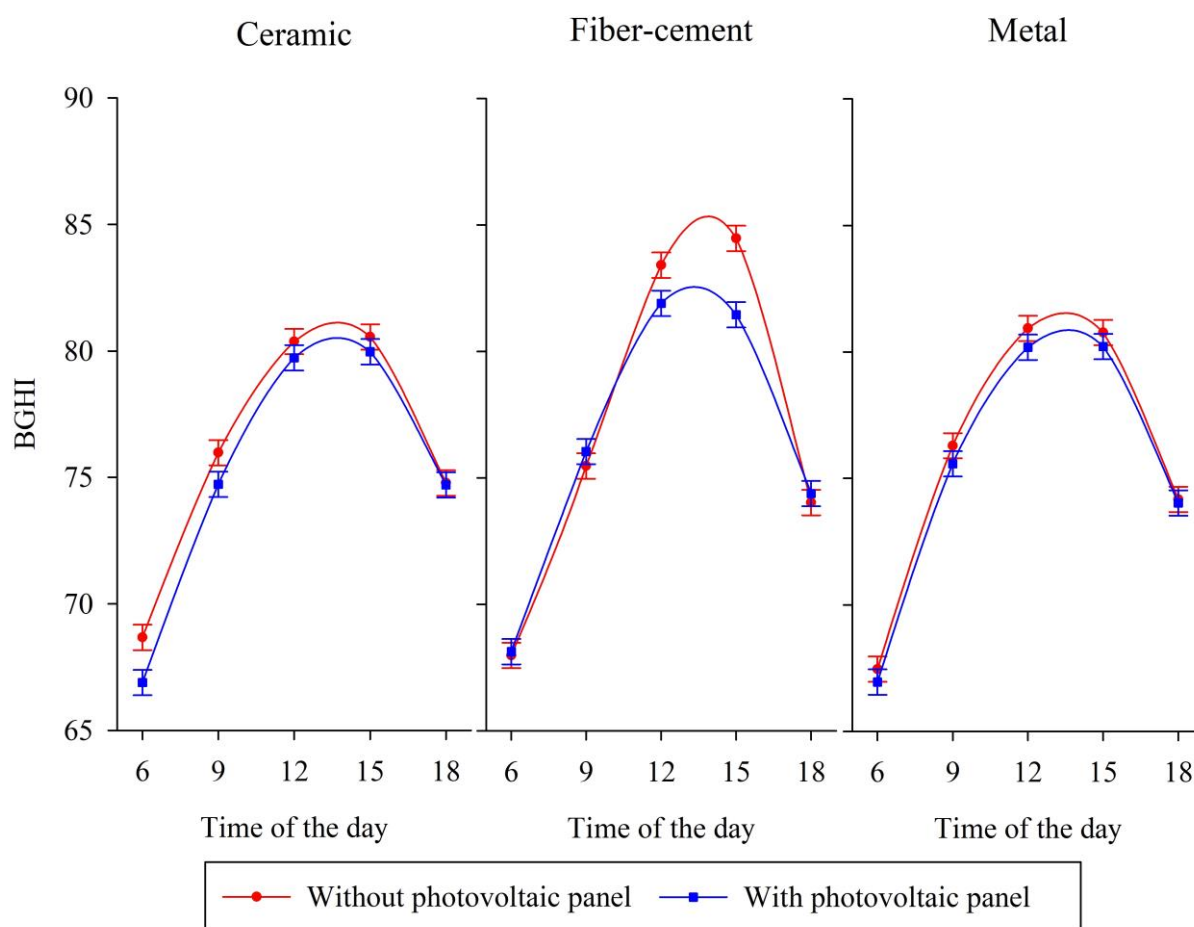

Figure 8. Behavior of the black and wet globe temperature index (BGHI) for the three types of tiles, with the presence and absence of the photovoltaic panel for ceramic, fiber-cement, and metallic tiles.

For the prototype with a ceramic roof, the calculated values of BGHI were 80.3 and 80.5 at 12:00 and 15:00 h, respectively (Figure 8). In the prototypes with the association of ceramic tile with a photovoltaic panel, the calculated values of BGHI were 79.7 at 12:00 h and 79.9 at 15:00 h. Thus, there is a reduction of about 0.6 in the BGHI for both times.

The highest calculated values of BGHI (Figure 8) were observed in the prototype with fiber-cement roofs, being 83.4 at 12:00 h and 84.4 at 15:00 h. In the association of the fiber-cement tile with the photovoltaic panel, the calculated values of BGHI in the prototypes were 81.9 at 12:00 h and 81.4 at 15:00 h. Thus, the differences observed between the absence and presence of the photovoltaic panel in the prototypes with fiber-cement roofs were about 1.5 at 12:00 h and about 3.0 at 15:00 h.

In the prototypes with metallic cover, the calculated values of BGHI were 80.9 at 12:00 h and 80.7 at 15:00 h, when associated with the photovoltaic panel these values were 80.1 and 80.2, respectively (Figure 8). In the prototypes with this type of tile, the application of the photovoltaic panel resulted in a reduction of about 0.75 at 12:00 h and about 0.60 at 15:00 h.

These high BGHI values verified in the hottest hours of the day (Figure 8) indicate that the thermal environment of all analyzed prototypes presented values above the tolerable limit for broilers, with an ideal range of 69 to 77 [32,47,48]. High BGHI values reduce feed consumption and weight gain in broilers, causing damage mainly in the noble parts such as the breast (Table 2) [32].

3.2.3. Radiation Heat Load (RHL)

In the analysis of variance for the RHL, it was found that the behavior of the values was similar for the three types of tiles, in the comparison between the absence and the presence of the photovoltaic panel, with the RHL being significantly lower in the prototypes equipped with a photovoltaic panel on the roofs. Thus, the average RHL values for the absence and presence of a photovoltaic panel were 471 ± 1.5 and 467 ± 1.5 W/m^2, respectively, representing a difference of about 4 W/m^2 (*p*-value = 0.01). This is mainly due to the shading provided by the materials used on the roofs [18,21,36,49]. It was verified that there was an interaction between the types of tile and the time of day (*p*-value = 0.006), with the fiber-cement tile being significantly higher than the ceramic tile at 12:00 h, not differing from the metallic tile.

The behavior of the RHL values in the prototypes with the three types of tiles, with and without photovoltaic panel, are presented in Figure 9.
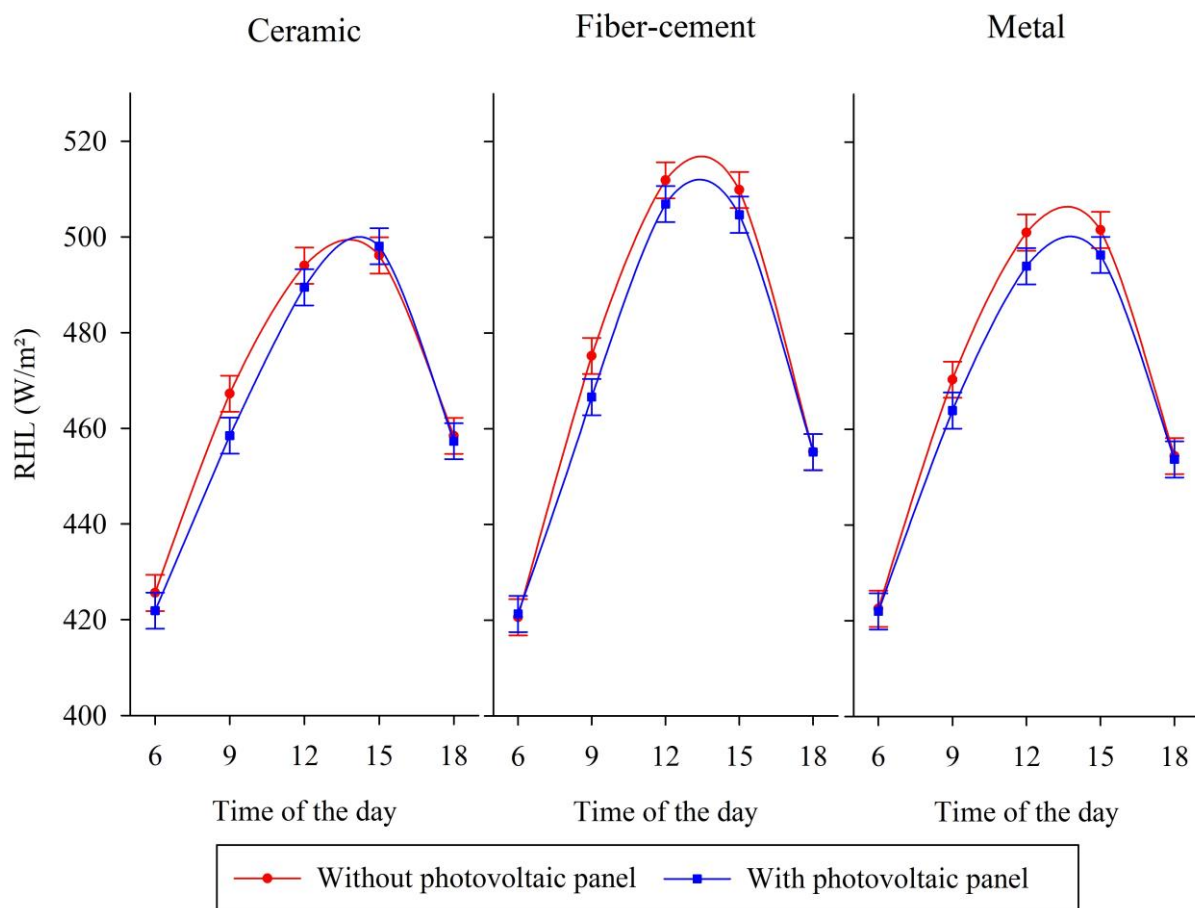

Figure 9. Behavior of the thermal radiation load (RHL) for the prototypes with the three types of tiles (ceramic, fiber-cement, and metallic) with and without the photovoltaic panel.

In the prototypes with ceramic roofs, the highest RHL values were observed at the hottest times of the day, being 494.00 W/m^2 at 12:00 h and 496.11 W/m^2 at 15:00 h, in the association of the ceramic tile with the photovoltaic panel these values were 489.49 W/m^2 and 498.04 W/m^2, for 12:00 and 15:00 h, respectively (Figure 9). A reduction of about 4.5 W/m^2 can be observed in the application of the photovoltaic panel. In ceramic roofs, the environment of the prototype with photovoltaic panel presented a RHL slightly higher than in the conventional one at 15:00 h; this can be explained by the ability of the ceramic tile to retain heat and slowly release it into the environment [36].

The highest RHL values were observed in the fiber-cement roof with the absence of the photovoltaic panel in the hottest hours of the day, being 511.94 W/m^2 at 12:00 h and 509.90 W/m^2 at 15:00 h (Figure 9). In the association of the fiber-cement tile with the photovoltaic panel, these values were 506.96 W/m^2 and 504.74 W/m^2, respectively. A difference of about 5.0 W/m^2 was observed at 12:00 h and about 5.2 W/m^2 at 15:00 h.

For the roof with metal tiles, the RHL was 501.12 W/m^2 at 12:00 h and 501.67 W/m^2 at 15:00 h, while in the metal roof with the photovoltaic panel it was 494.11 W/m^2 and 496.45 W/m^2, respectively. The differences are about 7.0 W/m^2 at 12:00 h and about 5.2 W/m^2 at 15:00 h (Figure 9).

In general, it was observed in the data presented that the application of photovoltaic panel to the roof of the prototypes confers a reduction in the air temperature, the BGHI and RHL for the three types of tiles tested, and a significant reduction in the THI for prototypes with fiber-cement tiles. This reduction is probably due to the decrease in the heat flow from the top to the bottom of the roof, which resulted in a lower amount of thermal radiation inside the prototypes. In the fiber cement roof, the photovoltaic panel acted as a second roof, which prevented the fiber-cement tile from absorbing radiation, improving the overall efficiency of the roof [50,51]. Similar results were found by [20,41] using photovoltaic panels in the coverage of small-scale prototypes.

However, the application of the photovoltaic panels on the roofs was not enough to keep the internal thermal environment within the comfort ranges, but the use of panels contributed to a considerable reduction in the amount of heat in the environments. This can represent a smaller mass of heat to be removed from the premises, which can generate a reduction in energy consumption by ventilation systems in real conditions. In this sense, in buildings with the application of photovoltaic panels, a significant reduction in the necessary cooling loads was observed, to maintain the environment in thermal comfort, with an annual net gain of about 3 to 4% [7].

Considering the poultry houses in Brazil, which require ventilation most of the time, a reduction in the amount of heat in the environment can generate savings in production, in addition to the photovoltaic systems offering energy autonomy to broiler producers.

4. Conclusions

The application of a photovoltaic panel on the roof of aviary prototypes, with a natural ventilation system, was able to reduce the air temperature by about 0.4 °C, the black globe humidity index by about 0.7, and the radiation heat load by about 4 W/m^2. This is statistically significant at the level $\alpha < 0.05$ for all tests.

In the prototypes with fiber-cement tiles, the application of photovoltaic panels was able to reduce the temperature and humidity index by about 4.8 in relation to the prototypes without the photovoltaic panel. This is statistically significant at the level $\alpha < 0.05$ for the test.

Although the presence of the photovoltaic panel on the roofs has not proved to be sufficient to promote thermal comfort inside the prototypes, for broilers in the fourth week of life, in the hottest hours of the day, their use significantly improved the indices of the thermal environment.

References

1. UNFCCC. Conference of the Parties. Adoption of the Paris Agreement. Proposal by the President; United Nations; 2015; FCCC/CP/2015/L.9/Rev.1; pp. 1–32. Available online: https://unfccc.int/documents/9064 (accessed on 10 October 2022).
2. Dos Santos, Í.P.; Rüther, R. The Potential of Building-Integrated (BIPV) and Building-Applied Photovoltaics (BAPV) in Single-Family, Urban Residences at Low Latitudes in Brazil. *Energy Build.* **2012**, *50*, 290–297. [CrossRef]
3. Singh, D.; Chaudhary, R.; Karthick, A. Review on the Progress of Building-Applied/Integrated Photovoltaic System. *Environ. Sci. Pollut. Res.* **2021**, *28*, 47689–47724. [CrossRef] [PubMed]
4. Santos, P.A.; Yanagi Junior, T.; Teixeira, V.H.; Ferreira, L. Ambiente Térmico No Interior de Modelos de Galpões Avícolas Em Escala Reduzida Com Ventilação Natural e Artificial Dos Telhados. *Eng. Agrícola* **2005**, *25*, 575–584. [CrossRef]
5. Tinôco, I. Avicultura Industrial: Novos Conceitos de Materiais, Concepções e Técnicas Construtivas Disponíveis Para Galpões Avícolas Brasileiros. *Rev. Bras. Cienc. Avic.* **2001**, *3*, 1–26. [CrossRef]
6. Awan, A.B.; Alghassab, M.; Zubair, M.; Bhatti, A.R.; Uzair, M.; Abbas, G. Comparative Analysis of Ground-Mounted vs. Rooftop Photovoltaic Systems Optimized for Interrow Distance between Parallel Arrays. *Energies* **2020**, *13*, 3639. [CrossRef]
7. Kapsalis, V.; Karamanis, D. On the Effect of Roof Added Photovoltaics on Building's Energy Demand. *Energy Build.* **2015**, *108*, 195–204. [CrossRef]
8. Shen, L.; Li, H.; Guo, L.; He, B.-J. Thermal and Energy Benefits of Rooftop Photovoltaic Panels in a Semi-Arid City during an Extreme Heatwave Event. *Energy Build.* **2022**, *275*, 112490. [CrossRef]
9. Bhuvad, S.S. Udayraj Investigation of Annual Performance of a Building Shaded by Rooftop PV Panels in Different Climate Zones of India. *Renew. Energy* **2022**, *189*, 1337–1357. [CrossRef]
10. Abuseif, M.; Gou, Z. A Review of Roofing Methods: Construction Features, Heat Reduction, Payback Period and Climatic Responsiveness. *Energies* **2018**, *11*, 3196. [CrossRef]
11. Dehwah, A.H.A.; Krarti, M. Energy Performance of Integrated Adaptive Envelope Systems for Residential Buildings. *Energy* **2021**, *233*, 121165. [CrossRef]
12. Espino-Reyes, C.A.; Ortega-Avila, N.; Rodriguez-Muñoz, N.A. Energy Savings on an Industrial Building in Different Climate Zones: Envelope Analysis and PV System Implementation. *Sustainability* **2020**, *12*, 1391. [CrossRef]
13. Dominguez, A.; Kleissl, J.; Luvall, J.C. Effects of Solar Photovoltaic Panels on Roof Heat Transfer. *Sol. Energy* **2011**, *85*, 2244–2255. [CrossRef]
14. Dang, H.A.; Nguyen, T.K. Impacts of Roof-Top Solar Photovoltaic Modules on Building Energy Performance: Case Study of a Residence in HCM City, Vietnam. *IOP Conf. Ser. Earth Environ. Sci.* **2020**, *505*, 012014. [CrossRef]
15. Pandiaraj, S.; Abdul Jaffar, A.; Muthusamy, S.; Panchal, H.; Pandiyan, S. A Study of Solar Heat Gain Variation in Building Applied Photovoltaic Buildings and Its Impact on Environment and Indoor Air Quality. *Energy Sources Part A Recovery Util. Environ. Eff.* **2022**, *44*, 6192–6212. [CrossRef]
16. Rahmani, F.; Robinson, M.A.; Barzegaran, M.R. Cool Roof Coating Impact on Roof-Mounted Photovoltaic Solar Modules at Texas Green Power Microgrid. *Int. J. Electr. Power Energy Syst.* **2021**, *130*, 106932. [CrossRef]
17. Singh, D.; Chaudhary, R. Impact of Roof Attached Photovoltaic Modules on Building Material Performance. *Mater. Today Proc.* **2021**, *46*, 445–450. [CrossRef]
18. Baêta, F.; Souza, C. *Ambiência Em Edificações Rurais*, 2nd ed.; Editora UFV: Viçosa, Brazil, 2010; Volume 1, ISBN 9788572693936.
19. Damasceno, F.A.; Shiassi, L.; Yanagi Junior, T.; Osorio Saraz, J.A.; de Oliveira, J.L. Evaluación Térmica de Tejas Ecologicas En Modelos Físicos de Galpones Avicolas. *Dyna* **2016**, *83*, 114. [CrossRef]

20. Bilčík, M.; Božiková, M.; Čimo, J. Influence of Roof Installation of PV Modules on the Microclimate Conditions of Cattle Breeding Objects. *Appl. Sci.* **2021**, *11*, 2140. [CrossRef]

21. Carneiro, T.A.; Guiselini, C.; Pandorfi, H.; Lopes Neto, J.P.; Loges, V.; Souza, R.F.L. de Condicionamento Térmico Primário de Instalações Rurais Por Meio de Diferentes Tipos de Cobertura. *Rev. Bras. De Eng. Agrícola E Ambient.* **2015**, *19*, 1086–1092. [CrossRef]

22. Maia, A.S.C.; de AndradeCulhari, E.; Fonsêca, V.D.F.C.; Milan, H.F.M.; Gebremedhin, K.G. Photovoltaic Panels as Shading Resources for Livestock. *J. Clean. Prod.* **2020**, *258*, 120551. [CrossRef]

23. Jentzsch, R.; Baêta, F.d.C.; Tinôco, Í.d.F.; Damasceno, F.A.; Cecon, P.R.; Saraz, J.A.O. Predição de Parametros Térmicos Ambientais No Interior de Modelos Físicos Em Escalas Reduzidas de Galpões Avícolas. *Interciencia* **2011**, *36*, 738–742.

24. Murphy, G. *Similitude in Engineering*; The Tonald Press Company: New York, NY, USA, 1950.

25. Eckelkamp, E.A.; Taraba, J.L.; Akers, K.A.; Harmon, R.J.; Bewley, J.M. Sand Bedded Freestall and Compost Bedded Pack Effects on Cow Hygiene, Locomotion, and Mastitis Indicators. *Livest. Sci.* **2016**, *190*, 48–57. [CrossRef]

26. Cassuce, D.C.; Tinôco, I.d.F.F.; Baêta, F.C.; Zolnier, S.; Cecon, P.R.; VIeira, M.d.F.A. Thermal Comfort Temperature Update for Broiler Chickens up to 21 Days of Age. *Eng. Agrícola* **2013**, *33*, 28–36. [CrossRef]

27. Abreu, V.M.N.; Abreu, P.G. Os Desafios Da Ambiência Sobre Os Sistemas de Aves No Brasil. *Rev. Bras. De Zootec.* **2011**, *40*, 1–14.

28. Thom, E.C. The Discomfort Index. *Weatherwise* **1959**, *12*, 57–61. [CrossRef]

29. Buffington, D.E.; Collazo-Arocho, A.; Canton, G.H.; Pitt, D.; Thatcher, W.W.; Collier, R.J. Black Globe-Humidity Index (BGHI) as Comfort Equation for Dairy Cows. *Trans. ASAE* **1981**, *24*, 0711–0714. [CrossRef]

30. Kelly, C.F.; Bond, T.E.; Ittner, N.R. Thermal Desing of Livestock Shades. *Agric. Eng.* **1950**, *31*, 601–606.

31. da Silva, E.T.; Leite, D.G.; Manabu Yuri, F.; Nery, F.d.S.G.; Rego, J.C.C.; Zanatta, R.d.A.; dos Santos, S.A.; Moura, V.V. Determinação Do Índice de Temperatura e Umidade (ITU) Para Produção de Aves Na Mesorregião Metropolitana de Curitiba—PR. *Rev. Acadêmica Ciência Anim.* **2004**, *2*, 47. [CrossRef]

32. de Oliveira, R.F.M.; Donzele, J.L.; de Abreu, M.L.T.; Ferreira, R.A.; Vaz, R.G.M.V.; Cella, P.S. Efeitos Da Temperatura e Da Umidade Relativa Sobre o Desempenho e o Rendimento de Cortes Nobres de Frangos de Corte de 1 a 49 Dias de Idade. *Rev. Bras. De Zootec.* **2006**, *35*, 797–803. [CrossRef]

33. R Core Team. *R: A Language and Environment for Statistical Computing*; 4.0.4 "Los.; R Foundation for Statistica Computing: Viena, Ausria, 2021.

34. Pinheiro, J.C.; Bates, D.M. *Mixed-Effects Models in S and S-PLUS*, 1st ed.; Springer, Ed.; Statistics and Computing; Springer: New York, NY, USA, 2000; ISBN 0-387-98957-9.

35. Santos, R.C.; Tinôco, I.d.F.F.; de Paulo, M.O.; Cordeiro, M.B.; Silva, J.N. da Análise de Coberturas Com Telhas de Barro e Alumínio, Utilizadas Em Instalações Animais Para Duas Distintas Alturas de Pé-Direito. *Rev. Bras. De Eng. Agrícola E Ambient.* **2002**, *6*, 142–146. [CrossRef]

36. Sampaio, C.A.d.P.; Cardoso, C.O.; de Souza, G.P. Temperaturas Superficiais de Telhas e Sua Relação Com o Ambiente Térmico. *Eng. Agrícola* **2011**, *31*, 230–236. [CrossRef]

37. da Silva, M.G.; Martin, S.; Oliveira, C.E.G.; Moscon, E.S.; Damasceno, F.A. Desempenho Térmico de Tipos de Cobertura No Interior de Modelos Reduzido de Galpões Avícolas. *Energ. Agric.* **2015**, *30*, 269. [CrossRef]

38. Fiorelli, J.; da Fonseca, R.; Morceli, J.A.B.; Dias, A.A. Influência de Diferentes Materiais de Cobertura No Conforto Térmico de Instalações Para Frangos de Corte No Oeste Paulista. *Eng. Agrícola* **2010**, *30*, 986–992. [CrossRef]

39. Sevegnani, K.B.; Ghelfi Filho, H.; da Silva, I.J.O. Comparação de Vários Materiais de Cobertura Através de Índices de Conforto Térmico. *Sci. Agric.* **1994**, *51*, 1–7. [CrossRef]

40. Lima, K.R.d.S.; Alves, J.A.K.; Araújo, C.V.; Manno, M.C.; de Jesus, M.L.C.; Fernandes, D.L.; Tavares, F. Avaliação Do Ambiente Térmico Interno Em Galpões de Frango de Corte Com Diferentes Materiais de Cobertura Na Mesorregião Metropolitana de Belém. *Rev. De Ciências Agrárias Amazon. J. Agric. Environ. Sci.* **2009**, *51*, 37–50.

41. Bonifacius, N.; Ekasiwi, S.N.N. Small Scale Experiment: Thermal Performance Comparison Between Fiber-Cement Roof and Photovoltaic Roof in Malang, Indonesia. *Makara J. Technol. Ser.* **2013**, *16*, 99–102. [CrossRef]

42. Xing, W.; Zhou, J.; Feng, Z. Effects of Mounting Geometries on Photovoltaic Module Performance Using CFD and Single-Diode Model. *Sol. Energy* **2014**, *103*, 541–549. [CrossRef]

43. Brinkworth, B.J.; Cross, B.M.; Marshall, R.H.; Yang, H. Thermal Regulation of Photovoltaic Cladding. *Sol. Energy* **1997**, *61*, 169–178. [CrossRef]

44. Chow, T.T. A Review on Photovoltaic/Thermal Hybrid Solar Technology. *Appl. Energy* **2010**, *87*, 365–379. [CrossRef]

45. Skoplaki, E.; Palyvos, J.A. On the Temperature Dependence of Photovoltaic Module Electrical Performance: A Review of Efficiency/Power Correlations. *Sol. Energy* **2009**, *83*, 614–624. [CrossRef]

46. Rivero, R. *Arquitetura e Clima: Acondicionamento Térmico Natural*, 1st ed.; Luzzatto Editores: Porto Alegre, Brazil, 1985.

47. Medeiros, C.M.; Baêta, F.d.C.; Oliveira, R.F.M.; Tinôco, I.d.F.F.; Albino, L.F.T.; Cecon, P.R. Efeitos Da Temperatura, Umidade Relativa e Velocidade Do Ar Em Frangos de Corte. *Eng. Agric.* **2005**, *13*, 277–286.

48. Queiroz, M.L.d.V.; Barbosa Filho, J.A.D.; Sales, F.A.d.L.; de Lima, L.R.; Duarte, L.M. Spatial Variability in a Broiler Shed Environment with Fogging System. *Resvista Ciência Agronômica* **2017**, *48*, 586–595. [CrossRef]

49. Furtado, D.A.; de Azevedo, P.V.; Tinôco, I.d.F.F. Análise Do Conforto Térmico Em Galpões Avícolas Com Diferentes Sistemas de Acondicionamento. *Rev. Bras. De Eng. Agrícola E Ambient.* **2003**, *7*, 559–564. [CrossRef]

50. Tuck, N.W.; Zaki, S.A.; Hagishima, A.; Rijal, H.B.; Yakub, F. Affordable Retrofitting Methods to Achieve Thermal Comfort for a Terrace House in Malaysia with a Hot–Humid Climate. *Energy Build.* **2020**, *223*, 110072. [CrossRef]
51. Zingre, K.T.; Wan, M.P.; Wong, S.K.; Toh, W.B.T.; Lee, I.Y.L. Modelling of Cool Roof Performance for Double-Skin Roofs in Tropical Climate. *Energy* **2015**, *82*, 813–826. [CrossRef]